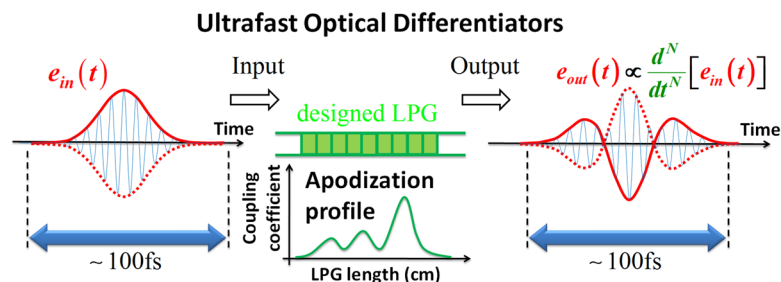# Ultrafast Optical Arbitrary-Order Differentiators Based on Apodized Long-Period Gratings

Reza Ashrafi, Student Member, IEEE
Mohammad H. Asghari, Student Member, IEEE
José Azaña, Member, IEEE

Ultrafast Optical Differentiators

Ultrafast Optical Arbitrary-Order Differentiators Based on Apodized Long-Period Gratings

Reza Ashrafi, *Student Member, IEEE,*
Mohammad H. Asghari, *Student Member, IEEE,* **and**
José Azaña, *Member, IEEE*

Institut National de la Recherche Scientifique, Energie, Matériaux et Télécommunications (INRS-EMT), Montréal, QC H5A 1K6, Canada

Abstract: We propose a novel, optimized design for arbitrary-order optical differentiation based on a uniform-period especially apodized long-period fiber or waveguide grating (LPG) operated in transmission. We show that the LPG solution can be optimized to utilize the entire grating resonance bandwidth for optical differentiation by properly customizing the LPG apodization profile through a discrete inverse-scattering grating synthesis technique. This strategy leads to a significantly increased processing speed and a maximized energetic efficiency as compared with previous unapodized LPG-based optical differentiator designs. As an example, optimized first-, second-, and third-order optical differentiators are designed using apodized LPGs implemented in standard single-mode fiber (SMF). The designed passive devices are practically feasible and offer an unprecedented operation bandwidth of 12 THz, which is capable of accurately processing time features as short as ∼100 fs, and an optimal energetic efficiency, which reaches a peak power spectral response of nearly 100% within their operation band.

Index Terms: Ultrafast optical signal processing, gratings, optical fiber devices, differentiation, inverse scattering algorithm.

1. Introduction

All-optical circuits for computing, information processing, and networking could overcome the severe speed limitations currently imposed by electronics-based systems [1], [2]. In this context, all-optical temporal differentiators are of fundamental interest as basic building blocks in ultrahigh-speed all-optical analog/digital signal processing and computing circuits [3]. We refer to an Nth-order optical differentiator (NOOD) as a device that provides the Nth-time derivative of the temporal complex envelope of an arbitrary input optical signal: the so-called field differentiators. Besides their intrinsic interest in future ultrafast all-optical computing and information processing circuits, these devices have been envisioned for various other applications of more immediate interest. To give a few relevant examples, first-order optical differentiators have proved useful for measurement and characterization of optical signals and devices [4]. Arbitrary-order optical differentiators have also been successfully employed for ultrashort optical pulse shaping, including generation of first- and higher order Hermite–Gaussian (HG) temporal waveforms from input Gaussian-like optical pulses [5]–[8]. These waveforms are particularly interesting in the context of optical telecommunications [9] and for advanced coding [7]–[9]. Some other important examples for applications of NOODs include

ultrashort flat-top pulse generation for use in the demultiplexing of 640-Gbit/s data in ultrahigh-speed transmission systems [10], ultrahigh bitrate ($\sim$Tbit/s) serial optical communication signals processing [11], optical dark-soliton detection [12], etc. In a more general framework, optical differentiators of different orders are necessary to create analog circuits that are capable of real-time computation of differential equations at ultrahigh speeds [13].

Notice that optical differentiator designs have been also demonstrated for processing real-positive time-domain intensity waveforms: the so-called intensity differentiators [14]–[19]. Intensity differentiators have been mostly used for microwave photonics applications [19]–[21]. These solutions are, however, outside the scope of our present work. This paper reports a new, advanced design for field differentiators (NOODs), providing a fully optimized performance. This design is based on the use of long-period waveguide or fiber gratings (LPGs).

It has been demonstrated that a uniform LPG operating in full-coupling condition implements a first-order time differentiator over a certain frequency bandwidth [5]. All-fiber implementations of this concept have enabled the demonstration of optical differentiators having an operation bandwidth (processing speed) in the THz range, i.e., capable of accurately processing optical waveforms with subpicosecond time features. In principle, an Nth-order differentiator could be realized by concatenating in series N single LPG devices; however, this would translate into a significantly reduced energetic efficiency and an increased implementation complexity. For instance, this solution requires the resonance frequencies of all N concatenated first-order differentiators to coincide precisely. Aiming at the implementation of higher order THz-bandwidth temporal differentiators based on LPGs, it has also been demonstrated that a uniform LPG incorporating $N - 1$ π-phase shifts can serve as an Nth-order temporal differentiator [22], [23]. As a main advantage, these mentioned LPG-based first- [5] and higher order [22], [23] differentiators operate in transmission mode (the input and output signals are carried by the same waveguide mode, e.g., core mode in a single-mode optical fiber). However, in these previous designs, only a fraction of the (destructive) transmission resonance bandwidth is employed for differentiation, i.e., typically the resonance bandwidth fraction over which the device's power spectral response keeps below $\sim$10% (assuming a 100% power transmission outside the passive device's resonance bandwidth). This limitation negatively affects two of the main performance specifications of these devices, namely its operation bandwidth, which is defined as the maximum input signal frequency bandwidth that can be accurately processed, and energetic efficiency, which is defined as the ratio between the output and input signal energy.

Field differentiators have also been demonstrated based on silicon microring resonator [24] and fiber Bragg gratings (FBGs) working in reflection [25], [26] or transmission [6], [27]. While these devices can be designed to achieve a fully optimized energetic efficiency, their bandwidth is typically limited to a few hundreds of gigahertz, which is capable of accurately processing time features at least a few picoseconds long.

In this paper, we propose and numerically demonstrate the use of a properly customized grating apodization profile along the length of an LPG to ensure that the entire resonance bandwidth of the device's transmission response can be used for optical differentiation. This translates into two key improvements, as compared with conventional unapodized LPG-based differentiators: The device's energetic efficiency is maximized while simultaneously increasing its processing speed. Apodization profiles for NOODs up to the third order, implemented in an optical fiber, are designed and numerically tested here for the first time to our knowledge. A discrete inverse scattering algorithm (DISA) [28] has been used to obtain the necessary LPG apodization profiles. To fairly compare the performance of our designs with those reported in previous works [5], [22], [23], we consider the same optical waveguide platform [standard single-mode fiber (SMF)] with identical fabrication constraints (peak coupling strength). The peak power spectral response (*PPSR*) from below $\sim$10% in previous designs [5], [22], [23] is improved to nearly 100% in our proposed designs (maximum possible for a passive device), resulting in a ten-fold increase in their energetic efficiency. In addition, the processing speed of the designed LPG differentiators is increased more than three times with respect to their unapodized counterparts, reaching unprecedented operation bandwidths > 10 THz.
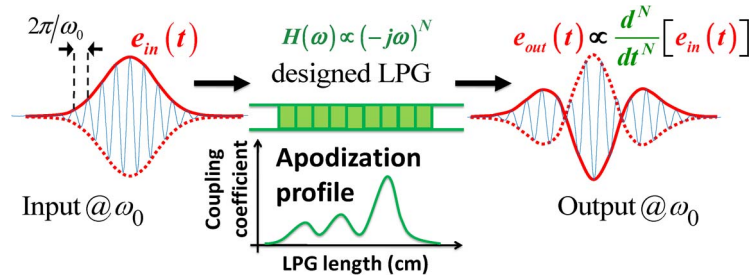
Fig. 1. Proposed architecture for the implementation of an optimized Nth-order all-optical LPG-based differentiator (output curve corresponds to $N = 2$).

The paper is structured as follows. In Section 2, the operation principle of an NOOD is presented. Section 3 is devoted to investigate the intrinsic processing speed and energetic efficiency limitations of previous LPG designs for optical differentiators [5], [22], [23], considering current fabrication technology constraints. In Section 4, our proposed designs based on all-fiber apodized LPGs for implementation of optimized NOODs ($N = 1, 2, 3$) are presented. In this section, we show the frequency-domain and time-domain simulation results for the proposed designs, demonstrating accurate processing of time features as short as $\sim$100 fs. The improvements offered by the newly proposed designs, as compared with previous LPG solutions, are also quantified and discussed. In Section 5, we evaluate in deeper detail the performance of the designed differentiators, using their maximum-to-minimum bandwidth ratio (*MMBR*) as a main figure of merit. Finally, Section 6 points out the conclusions of this work.

2. Operation Principle

An Nth-order optical temporal field differentiator (i.e., NOOD) is a linear filtering device that provides the Nth-order time derivative of the input pulse electric-field complex envelope. This device can be implemented using a linear optical filter with a spectral transfer function given by

$$H(\omega) \propto (-j\omega)^N \tag{1}$$

where ω is the angular baseband frequency [3] defined by $\omega = \omega_{opt} - \omega_0$, where ω_{opt} is the optical angular frequency variable, and ω_0 is the carrier angular frequency of the input optical signal. Also, the utilized variable *Frequency* or f hereafter, in the text or figures, is the baseband frequency defined as $f = \omega/2\pi$. According to (1), the amplitude spectral response of an NOOD is proportional to $|\omega|^N$ ($N = 1, 2, 3, 4, \ldots$). The spectral phase response for an even-order NOOD (i.e., $N = 2, 4, 6, \ldots$) has a linear profile (to account for the average propagation time through the device), and for an odd-order NOOD (i.e., $N = 1, 3, 5, \ldots$), it has an additional discrete π-phase shift at the NOOD's central frequency (i.e., $\omega = 0$) [5], [6]. Fig. 1 shows a schematic of the NOOD solution proposed in this work based on an all-fiber single-device LPG. As illustrated in Fig. 1, the LPG, to perform as a NOOD, is designed with a properly customized apodization profile. The output differentiated signal is obtained in the fiber core mode (i.e., same mode carrying the input optical signal).

As evidenced by the frequency transfer function in (1), an NOOD is essentially a notch optical filter (i.e., a band-stop filter). The notch-filtering characteristics that are intrinsic to LPGs working in transmission can then be customized to achieve the desired NOOD functionality. In particular, it has been previously shown that a uniform-period LPG designed to operate in full-coupling condition provides the spectral transfer function in (1) (for $N = 1$) over a certain fraction of its full resonance bandwidth [5]. Similarly, multiple-phase-shifted LPGs can be designed to achieve the transfer function in (1) for $N > 1$; again, this functionality is achieved only over a fraction of its full resonance bandwidth [22], [23]. In this paper, to use the entire resonance bandwidth of these LPG devices for the target differentiation operation, we introduce suitable grating apodization profiles, leading to the design of passive NOODs with maximum energetic efficiency and several times increased operation bandwidth.

3. Limitations of Previous LPG-Based Differentiators

3.1. Limitations of Uniform LPG-Based First-Order Differentiator

For consistency, in all the designs evaluated hereafter, we consider the same design parameters as in previously demonstrated LPG-based optical differentiators [5], [22], [23]. The assumed design considerations are as follows. The optical waveguide platform is considered to be a standard SMF (e.g., SMF-28). The grating period is $\Lambda = 415 \; \mu$m, which corresponds to coupling of the core mode into the fifth odd cladding mode at a central wavelength of 1535 nm. As previously derived for standard SMF [29], the following wavelength dependence was assumed for the effective refractive indices of the two coupled modes: $n_0(\lambda) = 1.46410 - 0.00830(\lambda - 1.555) - 0.00185(\lambda - 1.555)^2$ for the core mode and $n_5(\lambda) = 1.45769 - 0.00507(\lambda - 1.555) - 0.002479(\lambda - 1.555)^2$ for the cladding mode, where λ is the wavelength variable in micrometers. The maximum coupling coefficient (MCC) that can be achieved in practice is assumed to be limited to $K \approx 240(1/$m$)$, which corresponds to a practically achievable effective refractive index modulation amplitude of $\Delta n \approx 1 \times 10^{-3}$ in standard SMF [30], [31].

As mentioned above, a uniform LPG with a length L and a constant coupling coefficient K, operating in full-coupling condition, i.e., with $K \cdot L = \pi/2$, can serve as an ultrafast optical first-order differentiator [5]. This device has been experimentally demonstrated to be able to provide a considerably large operation bandwidth, up to $\sim$2.4 THz in previously fabricated devices [5]. The maximum achievable processing bandwidth of this optical differentiator is ultimately limited by the presence of a slight nonlinear dispersion slope of the core and cladding modes, which starts to deform the resonance dip linear shape when a large bandwidth is considered using numerical simulations [5]. In any case, the operation bandwidth of this differentiator design is just a fraction of the whole resonance bandwidth of the LPG, and this resonance bandwidth is limited by the maximum achievable coupling coefficient (MCC). To be more concrete, the useful fraction of the LPG resonance bandwidth is typically quantified by limiting the maximum deviation (MD) of the LPG amplitude spectral transfer function around its resonance frequency with respect to the ideal transfer function of a first-order differentiator (namely, linear amplitude variation). We assume here the same $MD = 9\%$ as that considered in [5]. Our numerical simulations show that for the considered practically achievable MCC, i.e., $K \approx 240(1/$m$)$, the operation bandwidth of a LPG-based first-order differentiator implemented in a standard SMF is approximately $BW \approx 3.4$ THz. According to this previous design [5], to achieve a larger operation bandwidth of 12 THz (i.e., the same bandwidth considered in our following designs), the required coupling coefficient should be $K \approx 785.4(1/$m$)$, which is far higher than the considered MCC (indeed, it would be extremely challenging to achieve this coupling coefficient in a standard SMF platform using present LPG fabrication technologies [30]–[32]).

Fig. 2 shows our simulation result of the previous approach [5], presenting the amplitude spectral response of the target first-order differentiator based on a uniform LPG. Coupled-mode theory has been used to simulate this LPG device [33]. In order to achieve the desired 12-THz operation bandwidth, this LPG has a length of $L = 0.2$ cm and a coupling coefficient of $K = 785.4(1/$m$)$, as mentioned above. In addition to the fact that the required coupling coefficient is several times larger than the considered practically achievable MCC, the $PPSR$ over the operation bandwidth of this differentiator, according to the considered $MD = 9\%$ is below $\sim$10% (i.e., $PPSR = (0.29)^2 \times 100 = 8.4\%$), resulting in the anticipated additional limited energetic efficiency of the differentiator device.

3.2. Limitations of Multiple-Phase-Shifted LPG-Based Higher Order Differentiators

It has been demonstrated that a uniform LPG incorporating $N - 1$ π-phase shifts can serve as an Nth-order temporal differentiator [22], [23]. In particular, for the second-order differentiator, the LPG consists of two uniform grating segments with a single π-phase shift between them. The lengths of the two uniform grating segments must be in the ratio of $3 : 1$, i.e., $L_{\text{long}}/L_{\text{short}} = 3$, where L_{long} and
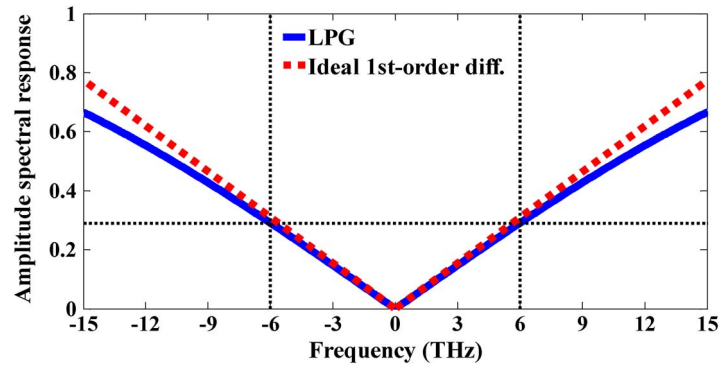
Fig. 2. Amplitude spectral response profile (solid blue curve) of a uniform LPG designed to implement a first-order differentiator with a customized operation bandwidth of 12 THz. According to the design considerations [5], the required coupling coefficient is $K = 785.4(1/m)$. Dashed red curve corresponds to the ideal first-order differentiator.

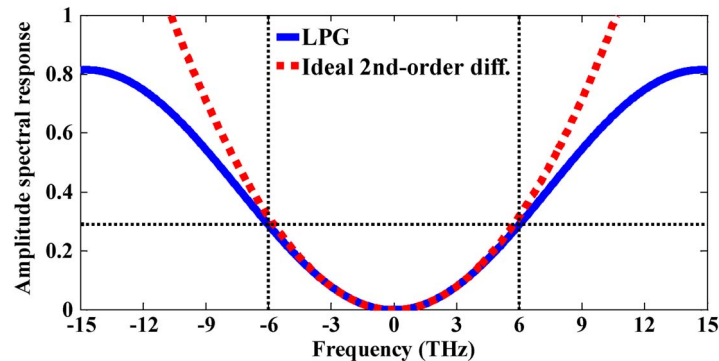
Fig. 3. Amplitude spectral response profile (solid blue curve) of a single π-phase shifted uniform LPG designed to implement second-order differentiator with a customized bandwidth of 12 THz. According to the design considerations [23], the required coupling coefficient is $K = 503(1/m)$. Dashed red curve corresponds to the ideal second-order differentiator.

L_{short} are the lengths of long and short uniform grating sections, respectively, and the coupling strength should be $K.L = \pi$ [22], where $L = L_{long} + L_{short}$ is the total LPG length.

The experimentally demonstrated single π-phase shifted uniform LPG-based second-order differentiator with an estimated operation bandwidth of 1.4 THz [23] had a length of $L = 65$ mm and a coupling coefficient of $K = 48.33(1/m)$. Our numerical simulation shows that for the considered practically achievable MCC, i.e., $K \approx 240(1/m)$, and the assumed $MD = 9\%$, the operation bandwidth of this second-order differentiator's design would be $\sim$5.3 THz. According to this previous approach [22], to achieve a larger operation bandwidth of 12 THz, the required coupling coefficient should be fixed to $K \approx 503(1/m)$, which is several times higher than the assumed MCC. The corresponding length is $L = 1.3$ cm. Fig. 3 shows the amplitude spectral response of the simulated second-order differentiator based on a single π-phase shifted uniform LPG [22] with an operation bandwidth of 12 THz. Coupled-mode theory combined with a transfer-matrix method has been used to simulate this device [33]. As for the case of first-order differentiator, the *PPSR* of this second-order differentiator is also below $\sim$10%.

4. Design of Apodized LPG-Based NOODs With Optimized Performance

In our proposed scheme for NOODs, a customized apodization is introduced along the LPG profile to optimize the device so that it provides the spectral response of the target NOOD, as defined by (1),
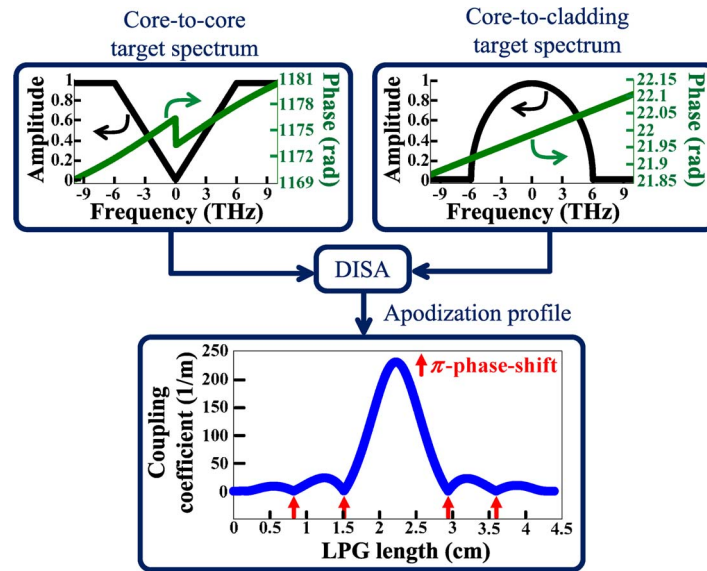
Fig. 4. Schematic of our design strategy based on the use of DISA [28] to obtain the LPG apodization profile for implementation of NOODs in core-to-core operation mode of the LPGs. The presented target spectra and apodization profile correspond to $N = 1$ (i.e., first-order differentiator).

over its entire transmission resonance bandwidth (core-to-core operation). This translates into the two key improvements anticipated above, namely an increased processing speed and a maximized energetic efficiency. Our proposed design approach for NOODs in this paper enables us to process optical signals with temporal features as short as ~100 fs, which is well beyond the reach of previously demonstrated all-fiber LPG-based NOODs, using practically feasible fabrication specifications.

In order to obtain the needed LPG apodization profiles, we have implemented a synthesis program tool based on a DISA [28]. Grating-assisted codirectional couplers, including LPGs, have been also designed by use of the Gel'fand–Levitan–Marchenko (GLM) inverse-scattering method to achieve a desired (target) linear filtering spectral response [34]–[36]. The GLM method is exact when the spectral response is expressed or approximated by rational functions, but it suffers from high algorithm complexity [28]. Generally, in our design cases, GLM could be used as well to synthesize the LPGs, but the DISA has a lower algorithm complexity and a simpler implementation scheme compared with the GLM method (e.g., in DISA there is no need to express the target spectral response as a rational function) [28].

We have considered all the same design parameters as in the previously demonstrated LPG-based differentiator [22], as defined in Section 3.1. Fig. 4 shows a schematic of our design strategy based on the use of DISA to obtain the LPG apodization profile. As illustrated in Fig. 4, the DISA synthesis program for LPG [18] allows one to obtain the corresponding apodization profile from the two target complex-field spectra, namely the core-to-cladding and core-to-core spectral transfer functions. Since the target NOOD functionality is implemented in the core-to-core transfer function of the LPG, leading to a more practical solution, the amplitude and phase profiles of the core-to-core target spectrum are entirely determined by the target NOOD's spectral response, as defined by (1). An operation bandwidth of 12 THz is considered for the NOODs in the core-to-core target spectrum. The amplitude profile of the core-to-cladding target spectrum is fixed by the well-known relationship $|H_{Cl}(f)| = (1 - |H_{Co}(f)|^2)^{1/2}$, where $|H_{Cl}(f)|$ and $|H_{Co}(f)|$ are the amplitude profiles of the core-to-cladding and core-to-core target spectra, respectively. The phase profile of the core-to-cladding target spectrum can be fixed arbitrarily in such a way that for each specific chosen phase profile, a different apodization profile is obtained. In the design cases reported in this work, we have considered a linear phase profile for the core-to-cladding target spectrum as we have observed that this choice translates into simpler (e.g., smoother) apodization
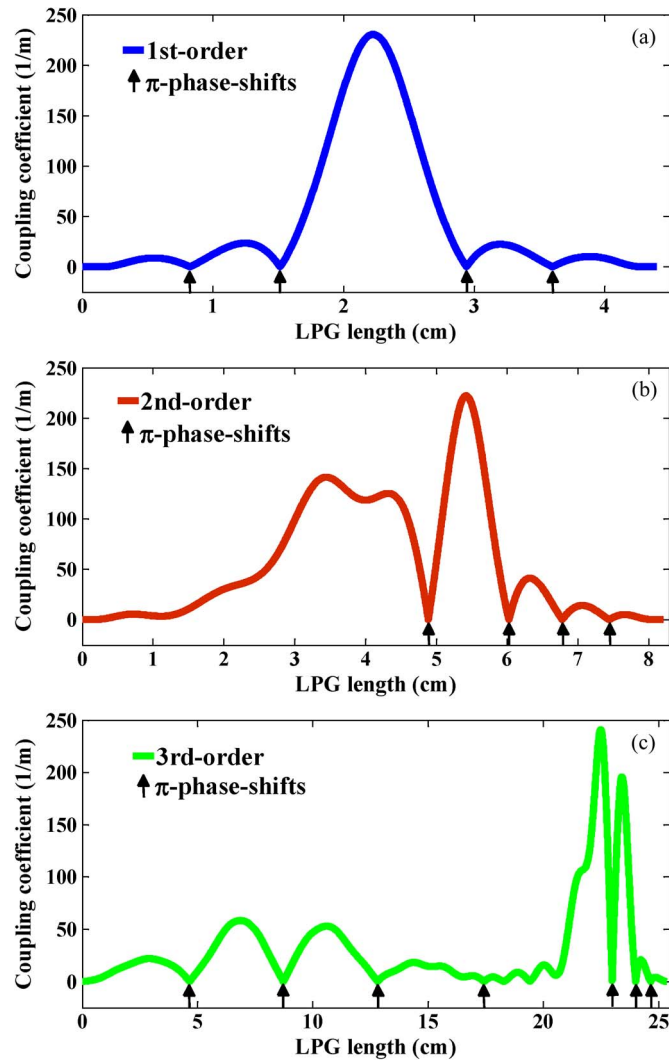
Fig. 5. Designed apodization profile for the optimized 12-THz bandwidth single-unit (a) first-, (b) second- and (c) third-order LPG-based all-optical differentiators.

profiles, while avoiding variations in the grating period, minimizing the required number of π-phase shifts along the grating profile, minimizing the peak coupling coefficient, and shortening the required LPG length.

Fig. 5(a)–(c) shows the obtained apodization profiles from our synthesis program tool for first-, second-, and third-order differentiators. The designed LPGs for first-, second- and third-order differentiators have lengths of 4.40 cm, 8.21 cm, and 25.35 cm, respectively (truncated from the originally obtained designs). The peak coupling coefficient of the obtained apodization profiles for the first-, second-, and third-order differentiators are 230.3(1/m), 222(1/m), and 240.8(1/m), respectively. These obtained values satisfy the above given practical constraint MCC < 240(1/m) while being significantly lower than those required to achieve the same target operation bandwidth using previous approaches [5], [22], [23]; see the results in Section 3.

LPGs are usually fabricated by a period-by-period technique [32]. A programmable shutter and aperture device are responsible for controlling the power, shape, and exposure time of the laser beam, and a translation stage moves the fiber point-by-point to write the apodization profile along the fiber. The shutter and the translation stage can be programmed in such a way that any type of uniform and nonuniform (e.g., apodized or chirped) LPG structure can be manufactured in an SMF
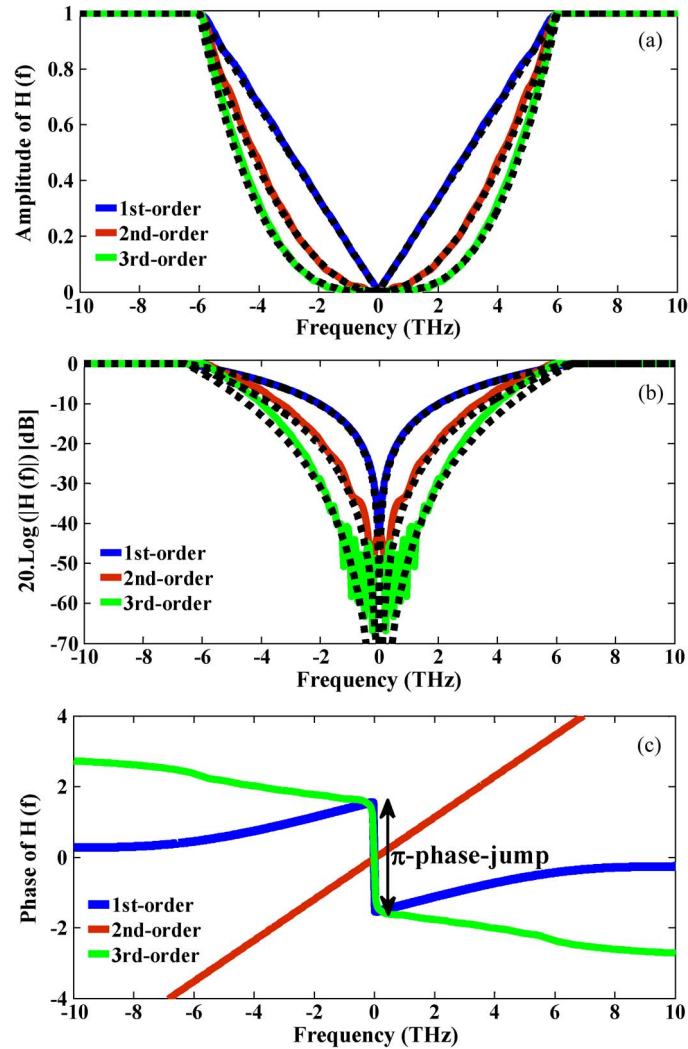
Fig. 6. Corresponding spectral amplitude in linear scale (a), spectral power in dB scale (b), and spectral phase (c) responses of the designed optimized 12-THz bandwidth first-, second-, and third-order LPG-based all-optical differentiators. The ideal spectral amplitude and spectral power responses in each case are shown with a dotted curves (the ideal spectral power response in dB scale (b) in each case at central frequency goes to minus infinity).

[32]. As it can be seen in Fig. 5, the shortest lobes of the obtained apodization profiles have a length of ∼1 cm, which can be practically fabricated with a resolution > 24 (i.e., 1 cm/415 μm) periods for each of these short lobes. Although the presented design in Fig. 5(c) shows the possibility for implementing the 12-THz bandwidth third-order differentiator with the considered practical MCC, fabrication of an LPG with a 25.35-cm length may be practically challenging.

    The spectral responses of the designed apodized LPGs were numerically simulated using coupled mode theory combined with a transfer matrix method [33]. Fig. 6(a)–(c) shows the simulated spectral amplitude and phase responses of the designed LPG profiles. Considering that a theoretical ideal zero (which corresponds to minus infinity in dB scale) in the transfer function $H(f)$ of these physical filters is practically impossible, the depth of the transmission resonance of such filters should be specified and imposed in the corresponding target spectral amplitude. The depth of the spectral response is defined as $d = 20 \times \log(|H(f_0)|)$ or $d = 10 \times \log(|P(f_0)|)$, where $H(f_0)$ and $P(f_0)$ are the amplitude and power spectral responses of the filter, respectively, at the central resonance frequency f_0 (i.e., $\omega_0/2\pi$), and log is the base-10 logarithm function. The experimental
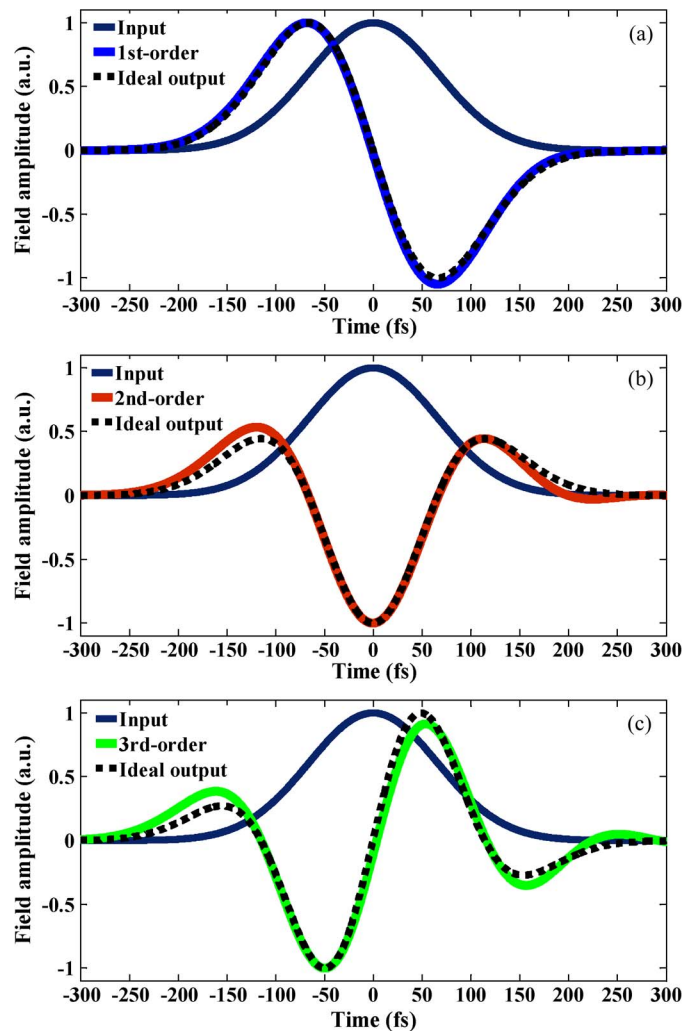
Fig. 7. Temporal responses (complex envelopes) of the designed optimized 12-THz bandwidth differentiators to a Gaussian optical input pulse with temporal intensity FWHM duration of 110 fs for the first- (a), second- (b) and third- (c) order differentiators. In each case, the field amplitude of the ideal output is shown with a dashed curve.

implementation of all-fiber LPG-based filters [37] shows that a transmission depth of over -60 dB is practically possible with current grating fabrication technologies.

To obtain a reasonable performance (see Section 4), in the DISA process, we have targeted a spectral amplitude $|H(f)|$ with a resonance dip of -50 dB. Finally, after truncation of the original apodization profile (the apodization profiles shown in Fig. 5(a)–(c) are after truncation), this target resonance depth was reduced to ~ -43 dB LPG; see responses shown in Fig. 6(b). The simulated spectral amplitude responses in linear [Fig. 5(a)] and dB [Fig. 5(b)] scales clearly show that the designed fiber devices provide very nearly the required spectral response in each case over the entire LPG resonance bandwidth, reaching a nearly 100% peak power response inside the differentiation bandwidth. Also, in the spectral phase response [Fig. 6(c)], the π-phase shift at the differentiator's central frequency that is required for odd-order devices (i.e., first- and third-order differentiators) was also obtained, whereas no phase shift can be observed for the even-order (i.e., second-order) differentiator.

To confirm that the designed LPGs can operate as first-, second-, and third-order temporal differentiators over the target bandwidth of 12 THz, an ultrashort Gaussian optical pulse with a temporal intensity FWHM width of 110 fs was launched into the designed NOODs. Fig. 7(a)–(c)
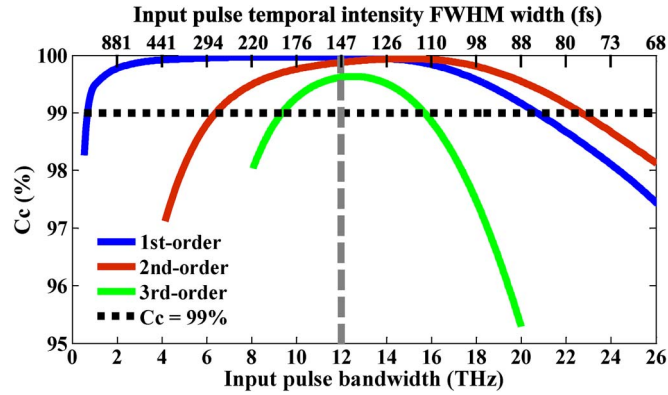
Fig. 8. Cross correlation coefficient of the designed devices for first-, second-, and third-order differentiators, assuming an input Gaussian pulse, which is used to estimate the *MMBR*.

shows the temporal responses of the designed NOODs ($N = 1$, 2, and 3) to the mentioned ultrashort Gaussian pulse. The generated time-domain outputs from the designed NOODs are in excellent agreement with the ideal first-, second-, and third-order differentiations of the input pulse shape, illustrating the capability of the proposed ultrafast signal processing devices to operate on optical signals in the femtosecond regime ($\sim$100 fs). As it will be investigated in deeper detail in Section 5, according to the results shown in Fig. 7 for the designed devices, the relative differentiation error increases as the differentiation order is increased [i.e., output waveforms from the designed second- and third-order differentiators, in Fig. 7(b) and (c), respectively, have a more significant deviation from the corresponding ideal waveforms, as compared with the output waveform from the first-order differentiator in Fig. 7(a)].

5. Performance Analysis

In this section, the performance of the designed differentiators is evaluated by estimating the output waveform similarity with respect to the corresponding ideal output over the target range of input pulse bandwidths. The mentioned similarity is estimated by using the cross-correlation coefficient (C_c) between the ideal output and simulated differentiator's output, which is defined as follows [38]

$$C_c = \frac{\int_{-\infty}^{+\infty} P_{out}(t)P_{ideal}(t)dt}{\sqrt{\left(\int_{-\infty}^{+\infty} P_{out}^2(t)dt\right)\left(\int_{-\infty}^{+\infty} P_{ideal}^2(t)dt\right)}} \times 100\% \tag{2}$$

where $P_{out}(t)$ and $P_{ideal}(t)$ are the time-domain intensity profiles of the simulated differentiator's output and the ideal output, respectively. The acceptable operation bandwidth range is defined by considering a minimum limit in the cross-correlation coefficient of the acceptable outputs, e.g., corresponding to $C_c > 99\%$. In relation with these metrics, we use the device's *MMBR* as a main figure of merit to evaluate the differentiator's performance.

The device's *MMBR* is expressed as the ratio between the upper (BW_{max}) and the lower (BW_{min}) limits of the acceptable operation bandwidth range

$$MMBR = \frac{BW_{max}}{BW_{min}}. \tag{3}$$

We recall that BW_{max} and BW_{min} are the minimum and maximum acceptable frequency bandwidths of the input pulse that correspond to the value of 99% in the cross-correlation coefficient. For estimation of the *MMBR*, a Gaussian input pulse is assumed. It should be noted that this shape exhibits a particularly poor performance concerning the cross-correlation coefficient value estimated from (2). This is due to the fact that one of the main practical deviations of a practical

TABLE 1

Maximum and minimum acceptable bandwidths of input pulse and *MMBRs* which show the broadness of the acceptable input pulse bandwidth range for each of the designed NOODs

Designed NOODs	First-order differentiator	Second-order differentiator	third-order differentiator
BW_{min}	680 GHz	6.40 THz	9.34 THz
BW_{max}	20.72 THz	22.70 THz	15.70 THz
MMBR	30.47	3.55	1.68

optical differentiator with respect to the ideal device's response concerns the limited depth of its spectral resonance dip (at the grating resonance frequency), and the Gaussian pulse energy is heavily concentrated around this resonance frequency. In what follows, the bandwidth of the input Gaussian pulse is considered to be the full width at 0.3981% of the amplitude spectrum peak. This bandwidth definition has been fixed to ensure that the peak of the resulting C_c curves is reached at approximately 12 THz, which is the nominal operation bandwidth of the designed NOODs.

Fig. 8 shows the numerically calculated cross-correlation coefficient versus the input pulse bandwidth for the designed NOODs. These curves are used to estimate the minimum and maximum acceptable frequency bandwidths of the input signal for each of the designed NOODs, as well as the corresponding device *MMBR*, as given in Table 1.

The estimated *MMBR* in each case shows the broadness of the acceptable input pulse bandwidth range. Performing a higher order differentiation needs a larger depth in the transfer function of the differentiator [39]. Therefore, assuming the same depth in the spectral responses of all NOODs ($N = 1, 2, 3$), we expect to have a shorter acceptable operation bandwidth range for higher order differentiators. All of the designed NOODs in this work have the same resonance depth (i.e., ~ -43 dB) in their spectral responses. Therefore, the results summarized in Table 1 are in good agreement with our theoretical expectations: The device's *MMBR* decreases as the differentiation order is increased.

6. Conclusion

We have reported an optimized design for passive LPG-based NOODs in which a customized apodization profile is introduced to achieve the desired differentiation response over the entire resonance bandwidth of the LPG. This translates into two key improvements in the devices' performance as compared with previous unapodized LPG designs, namely an increased operation bandwidth and a maximized energetic efficiency. The proposed strategy has been numerically proved by presenting practically feasible LPG designs for first-, second-, and third-order optical differentiators implemented in standard SMF offering an unprecedented operation bandwidth > 10 THz and with a fully improved energetic efficiency.

References

[1] J. Azaña, C. K. Madsen, K. Takiguchi, and G. Cincontti, Eds., "Special issue on 'Optical signal processing'," *J. Lightw. Technol.*, vol. 24, no. 7, pp. 2484–2486, Jul. 2006.

[2] C. K. Madsen, D. Dragoman, and J. Azaña, Eds., "Special issue on 'Signal analysis tools for optical signal processing'," *EURASIP J. Appl. Signal Process.*, no. 10, pp. 1449–1623, 2005.

[3] N. Q. Ngo, S. F. Yu, S. C. Tjin, and C. H. Kam, "A new theoretical basis of higher-derivative optical differentiators," *Opt. Commun.*, vol. 230, no. 1–3, pp. 115–129, Jan. 2004.

[4] F. Li, Y. Park, and J. Azaña, "Linear characterization of optical pulses with durations ranging from the picosecond to the nanosecond regime using ultrafast photonic differentiation," *J. Lightw. Technol.*, vol. 27, no. 21, pp. 2484–2767, Nov. 1, 2009.

[5] R. Slavík, Y. Park, M. Kulishov, R. Morandotti, and J. Azaña, "Ultrafast all-optical differentiators," *Opt. Express*, vol. 14, no. 22, pp. 10 699–10 707, Oct. 2006.

[6] L. M. Rivas, S. Boudreau, Y. Park, R. Slavík, S. LaRochelle, A. Carballar, and J. Azaña, "Experimental demonstration of ultrafast all-fiber high-order photonic temporal differentiators," *Opt. Lett.*, vol. 34, no. 12, pp. 1792–1794, Jun. 15, 2009.

[7] H. J. A. Da Silva and J. J. O'Reilly, "Optical pulse modeling with Hermite-Gaussian functions," *Opt. Lett.*, vol. 14, no. 10, pp. 526–528, May 15, 1989.

[8] M. H. Asghari and J. Azaña, "Proposal and analysis of a reconfigurable pulse shaping technique based on multi-arm optical differentiators," *Opt. Commun.*, vol. 281, no. 18, pp. 4581–4588, Sep. 2008.

[9] M. Stratmann, T. Pagel, and F. Mitschke, "Experimental observation of temporal soliton molecules," *Phys. Rev. Lett.*, vol. 95, no. 14, pp. 143902-1–143902-3, Sep. 2005.

[10] L. K. Oxenløwe, R. Slavík, M. Galili, H. C. H. Mulvad, A. T. Clausen, Y. Park, J. Azaña, and P. Jeppesen, "640 Gb/s timing jitter-tolerant data processing using a longperiod fiber-grating-based flat-top pulse shaper," *IEEE J. Sel. Topics Quantum Electron.*, vol. 14, no. 3, pp. 566–572, May/Jun. 2008.

[11] L. K. Oxenlwe, M. Galili, H. Hu, H. Ji, E. Palushani, J. L. Areal, J. Xu, H. C. H. Mulvad, A. T. Clausen, and P. Jeppesen, "Serial optical communications and ultra-fast optical signal processing of Tbit/s data signals," in *Proc. IEEE Top. Meeting MWP*, Montreal, QC, Canada, Oct. 5–9, 2010, pp. 361–364.

[12] N. Q. Ngo, L. N. Binh, and X. Dai, "Optical dark-soliton generators and detectors," *Opt. Commun.*, vol. 132, no. 3/4, pp. 389–402, Dec. 1996.

[13] J. Azaña, "Ultrafast analog all-optical signal processors based on fiber-grating devices," *IEEE Photon. J.*, vol. 2, no. 3, pp. 359–386, Jun. 2010.

[14] P. Velanas, A. Bogris, A. Argyris, and D. Syvridis, "High-speed all-optical first- and second-order differentiators based on cross-phase modulation in fibers," *J. Lightw. Technol.*, vol. 26, no. 18, pp. 3269–3276, Sep. 15, 2008.

[15] Z. Li and C. Wu, "All-optical differentiator and high-speed pulse generation based on cross-polarization modulation in a semiconductor optical amplifier," *Opt. Lett.*, vol. 34, no. 6, pp. 830–832, Mar. 15, 2009.

[16] Y. Park, M. H. Asghari, and J. Azaña, "Reconfigurable higher-order photonic intensity temporal differentiator," in *Proc. IEEE LEOS Annu. Meeting Conf.*, 2009, pp. 731–732.

[17] J. Zhou, S. Fu, S. Aditya, P. P. Shum, C. Lin, V. Wong, and D. Lim, "Photonic temporal differentiator based on polarization modulation in a LiNbO$_3$ phase modulator," in *Proc. IEEE Int. Top. Meeting MWP*, 2009, pp. 1–3.

[18] A. V. Okishev, "Optical differentiation and multimillijoule ∼150 ps pulse generation in a regenerative amplifier with a temperature-tuned intracavity volume Bragg grating," *Appl. Opt.*, vol. 49, no. 8, pp. 1331–1334, Mar. 10, 2010.

[19] J. Xu, X. Zhang, J. Dong, D. Liu, and D. Huang, "All-optical differentiator based on cross-gain modulation in semiconductor optical amplifier," *Opt. Lett.*, vol. 32, no. 20, pp. 3029–3031, Oct. 15, 2007.

[20] X. Li, J. Dong, Y. Yu, and X. Zhang, "A tunable microwave photonic filter based on an all-optical differentiator," *IEEE Photon. Technol. Lett.*, vol. 23, no. 5, pp. 308–310, Mar. 2011.

[21] J. Niu, K. Xu, X. Sun, Q. Lv, J. Dai, J. Wu, and J. Lin, "Instantaneous microwave frequency measurement using a photonic differentiator and an opto-electric hybrid implementation," in *Proc. APMP*, Hong Kong, Apr. 26–28, 2010.

[22] M. Kulishov, D. Krcmarík, and R. Slavík, "Design of terahertz-bandwidth arbitrary-order temporal differentiators based on long-period fiber gratings," *Opt. Lett.*, vol. 32, no. 20, pp. 2978–2980, Oct. 15, 2007.

[23] R. Slavík, Y. Park, M. Kulishov, and J. Azaña, "Terahertz-bandwidth high-order temporal differentiators based on phase-shifted long-period fiber gratings," *Opt. Lett.*, vol. 34, no. 20, pp. 3116–3118, Oct. 15, 2009.

[24] F. Liu, T. Wang, L. Qiang, T. Ye, Z. Zhang, M. Qiu, and Y. Su, "Compact optical temporal differentiator based on silicon microring resonator," *Opt. Express*, vol. 16, no. 20, pp. 15 880–15 886, Sep. 2008.

[25] M. Li, D. Janner, J. Yao, and V. Pruneri, "Arbitrary-order all-fiber temporal differentiator based on a fiber Bragg grating: Design and experimental demonstration," *Opt. Express*, vol. 17, no. 22, pp. 19 798–19 807, Oct. 2009.

[26] D. Gatti, T. T. Fernandez, S. Longhi, and P. Laporta, "Temporal differentiators based on highly-structured fibre Bragg gratings," *Electron. Lett.*, vol. 46, no. 13, pp. 943–945, Jun. 24, 2010.

[27] M. A. Preciado and M. A. Muriel, "Design of an ultrafast all-optical differentiator based on a fiber Bragg grating in transmission," *Opt. Lett.*, vol. 33, no. 21, pp. 2458–2460, Nov. 1, 2008.

[28] J. K. Brenne and J. Skaar, "Design of grating-assisted codirectional couplers with discrete inverse-scattering algorithms," *J. Lightw. Technol.*, vol. 21, no. 1, pp. 254–263, Jan. 2003.

[29] M. Kulishov and J. Azaña, "Long-period fiber gratings as ultrafast optical differentiators," *Opt. Lett.*, vol. 30, no. 20, pp. 2700–2702, Oct. 15, 2005.

[30] T. Erdogan, "Cladding-mode resonances in short- and long-period fiber grating filters," *J. Opt. Soc. Amer. A, Opt. Image Sci.*, vol. 14, no. 8, pp. 1760–1773, Aug. 1997.

[31] K. P. Chen, P. R. Herman, and R. Tam, "Strong fiber Bragg grating fabrication by hybrid 157- and 248-nm laser exposure," *IEEE Photon. Technol. Lett.*, vol. 14, no. 2, pp. 170–172, Feb. 2002.

[32] R. Kritzinger, D. Schmieder, and A. Booysen, "Azimuthally symmetric long-period fibre grating fabrication with a TEM$_{01}$-mode CO$_2$ laser," *Meas. Sci. Technol.*, vol. 20, no. 3, p. 034004, Mar. 2009.

[33] R. Kashyap, *Fiber Bragg Gratings*.   New York: Academic, 1999.

[34] K. A. Winick, "Design of grating-assisted waveguide couplers with weighted coupling," *J. Lightw. Technol.*, vol. 9, no. 11, pp. 1481–1492, Nov. 1991.

[35] G.-W. Chern and L. A. Wang, "Analysis and design of almost-periodic vertical-grating-assisted codirectional coupler filters with nonuniform duty ratios," *Appl. Opt.*, vol. 39, no. 25, pp. 4629–4637, Sep. 2000.

[36] G. H. Song, "Toward the ideal codirectional Bragg filter with an acoustooptic-filter design," *J. Lightw. Technol.*, vol. 13, no. 3, pp. 470–480, Mar. 1995.

[37] R. Slavík, "Extremely deep long-period fiber grating made with CO$_2$ laser," *IEEE Photon. Technol. Lett.*, vol. 18, no. 16, pp. 1705–1707, Aug. 15, 2006.

[38] A. Papoulis, *The Fourier Integral and its Applications*.   New York: McGraw-Hill, 1962.

[39] R. Ashrafi and J. Azaña, "Figure of merit for photonic differentiators," unpublished results.